HORIZONTAL BEAM-SIZE MEASUREMENTS AT CESR-TA USING SYNCHROTRON-LIGHT INTERFEROMETER*

S.T. Wang, J. Conway, M. Palmer, D. Hartill, D.L. Rubin, CLASSE, Cornell University, USA
R. Campbell, R. Holtzapple, CalPoly, USA

Abstract

A horizontal beam profile monitor utilizing visible synchrotron radiation from a bending magnet has been designed and installed in CESR. The monitor employs a double-slit interferometer which has been used to measure horizontal beam sizes over a wide range of beam currents. By varying the separation of the slits, beam sizes ranging from 50 to 500 μm can be measured with a resolution of approximately 5 μm. The method for extracting the horizontal beam size from the interference pattern is presented and its application to intrabeam scattering studies is described.

INTRODUCTION

Visible light from synchrotron radiation (SR) has been widely used to measure and monitor the transverse beam size in accelerators [1]. Because of the diffraction limit, depth of field, and many other factors, the direct imaging method cannot measure the transverse beam size very accurately when the beam size is comparable to or smaller than the optical resolution. For the CESR-TA low emittance lattice [2], the theoretical horizontal beam size at the source point of the visible beam size monitor (vBSM) is 154 μm (Table 1), which is below the calculated optical resolution (~230 μm) [3]. Therefore, the direct imaging method is not suitable for measuring the horizontal beam size in this lattice.

The SR interferometer first applied by Mitsuhashi [4] is a well developed instrument which has been constructed in many storage rings and x-ray facilities [1]. It was successfully demonstrated to accurately measure transverse beam sizes of less than 300 μm [5]. In this paper, we review the configuration of the interferometer developed in CESR and discuss its application to measure horizontal beam size and its calibration.

INTERFEROMETER

The principles behind the interferometer method have been discussed in many papers [1,4]. Here we briefly review the method. The SR interferometer is a wave-front-division-type two-beam interferometer using polarized quasi-monochromatic light. When the light intensities at two slits are the same, the interference pattern at the detector plane can be written as:

$$I(x) = I_0\left[\mathrm{sinc}\left(\frac{2\pi a}{\lambda R}x+\phi\right)\right]^2\left(1+|\gamma|\cos\left(\frac{2\pi D}{\lambda R}x+\psi\right)\right) \quad (1)$$

where I_0 is the light intensity through the slits, a is the slit width, R is the distance between the double slits and the detector, λ is the wavelength, and D is the separation between double slits. ϕ and ψ are phase shifts. γ denotes the spatial coherence (or visibility).

From the van Cittert-Zernicke theorem, the degree of coherence γ is the Fourier transform of the source distribution *f(x)*:

$$\gamma = \int dx f(x)\exp\left(-i\frac{2\pi D}{\lambda L}x\right) \quad (2)$$

where L is the distance between the source and the double slits. If the beam shape *f(x)* is a Gaussian profile, its width σ_x can be determined from the relation:

$$\sigma_x = \frac{\lambda L}{\pi D}\sqrt{\frac{1}{2}\ln\frac{1}{\gamma}} \quad (3)$$

Therefore, by acquiring and fitting the interference pattern to obtain the spatial coherence γ, we can measure the beam size σ_x.

Table 1: Twiss parameters at the vBSM source point

Energy [GeV]	2.085	η_x [m]	0.024
ε_x [nm-rad]	2.6	σ_E/E [%]	0.081
β_x [m]	9.2	σ_x [μm]	154

CESR-TA INTERFEROMETER

In order to measure the horizontal beam size accurately, a SR interferometer was constructed at the north area of CESR. Figure 1 shows the schematic layout of the instrument. The visible SR from a soft bending magnet was reflected by a Beryllium mirror in the vacuum chamber, which accepts light within a 2.5×2.2 mrad (H×V) aperture. Through an adjustable iris, the SR photons reach the double slits and a focusing lens (f=5m), which is 6 m from the source. Passing through many reflection mirrors, the SR light arrives at an optical table located about 27 m from the source. Then on the optical table, the SR light goes through a second lens (f=1m), a polarizer, a 500-nm narrow bandpass filter and reaches the CCD camera at last.

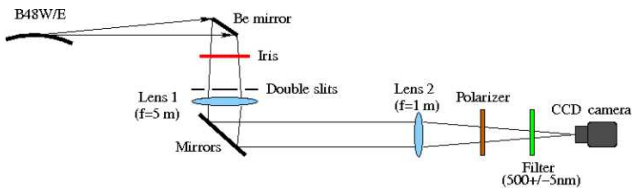

Figure 1: Layout of interferometer setup.

The iris opening is adjustable within the range 3.0~22 mm, which limits the acceptance of visible light down to 0.5 mrad and reduces the depth of field from 350 to 70 mm.

* Work supported by the National Science Foundation and Department of Energy under contract numbers PHY-0734867, PHY-1002467, PHYS-1068662, and DE-FC02-08ER41538, DE-SC0006505.

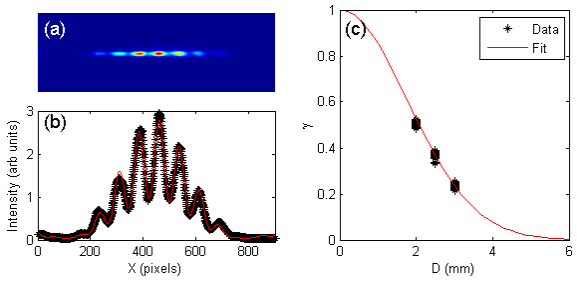

Figure 2: A typical horizontal beam size measurement.

Because the double slits are located inside the tunnel, adjustment of the slit separation is inconvenient during operation. Therefore, three vertically aligned double slits with fixed slit separation (D=2.0, 2.5, 3.0 mm) were machined in one piece and mounted on a motorized translation stage. Different sets of slits can be chosen to measure the horizontal beam size over different range.

A typical interference pattern measured with a set of double slits (D=2.0 mm) is shown in Fig. 2a. From fitting the fringes with Eq. 1, the visibility γ=0.52±0.01 was obtained (Fig. 2b), which yields σ_x=275±4 μm assuming a Gaussian distributed beam profile (Eq. 3). The visibilities using slits with three different separations were also obtained (Fig. 2c). By fitting the visibility as a function of slit separation, a more accurate horizontal beam size σ_x =272±1 μm was obtained, which is consistent with the measurement using one set of slits. Although the second method (scanning slit separation) yields more accurate beam size, it is not practical for monitoring the beam size, especially when the beam size changes rapidly. Therefore, the same set of slits was used to monitor the beam size during the intrabeam scattering (IBS) studies.

ERROR ANALYSIS

In order to obtain accurate beam size information, care must be taken to setup the interferometer correctly, especially to measure very small beam size. For example, the linearity of the CCD camera was checked to insure no intensity dependence of the camera [6]. The relative intensity on each of the slits needs to be checked to remove the intensity imbalance effect [4].

However, since the SR comes from a horizontal bending magnet, the effects due to the curvature of the trajectory and the depth of field are unavoidable systematic errors when measuring the horizontal beam size. Considering these effects, the visibility γ_h is then given by a superimposing integration of the van Cittert-Zernike theorem [4]:

$$\gamma_h = \iint \frac{2\sqrt{I_1(\psi)I_2(\psi)}}{I_1(\psi)+I_2(\psi)} f[x-\rho(1-\cos(\psi)),\psi]\, g(\psi)\exp(-i\frac{2\pi D}{\lambda L}x)\,d\psi dx \quad (4)$$

where $g(\psi)$ is the angular distribution of the SR beam in the horizontal plane as a function of the observation angle ψ, ρ is the bending radius; I_1 and I_2 are the intensities of the light that illuminate the double slits. Assuming the beam has a Gaussian profile:

$$f[x-\rho(1-\cos(\psi)),\psi] = \frac{1}{\sqrt{2\pi\sigma_x^{\,2}}}\exp\left[-\frac{(x-\rho(1-\cos\psi))^2}{2\sigma_x^{\,2}}\right] \quad (5)$$

the visibility function now becomes:

$$\gamma_h = \int \frac{2\sqrt{I_1(\psi)I_2(\psi)}}{I_1(\psi)+I_2(\psi)} g(\psi)\exp\left[-2(\frac{\pi D\sigma_x}{\lambda(L-\rho\sin\psi)})^2 - i\frac{2\pi D\rho(1-\cos\psi)}{\lambda(L-\rho\sin\psi)}\right] d\psi \quad (6)$$

From Eq. 6, the visibility as a function of the slit separation (D) and the beam size (σ_x) were both calculated assuming σ_x=220 μm and D=2.5 mm, respectively (Fig. 3). As we can see, the overall effect is small, consistent with the previous simulation [4]. The effect is negligible when σ_x is greater than 400 μm; but it becomes pronounced when σ_x is less than 100 μm. Based on the simulation results, the systematic error due to the nature of bending magnet can be corrected.

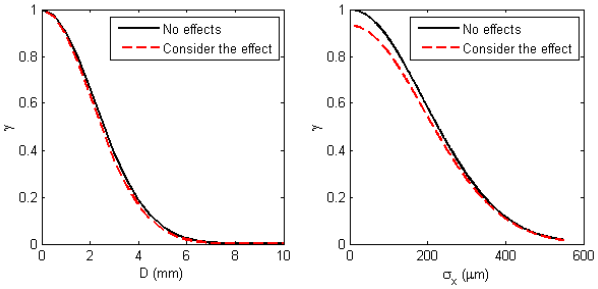

Figure 3: Simulated visibility as a function of D and σ_x ignoring (Eq. 2) and including depth of field (Eq. 6).

As noted above, the depth of field can be adjusted by varying the iris opening. The beam size was measured to be independent of depth of field over the range from 350 to 80 mm for a 250 μm beam, consistent with the results in Fig. 3.

In CESR, we have observed ~50 μm beam motion both horizontally and vertically. This beam jittering could generate phase shift in the interference pattern and reduce the visibility so that the measured beam size is larger than the actual beam size. Flanagan et al. have calculated the phase error when the beam is off the nominal orbit [7]:

$$\Delta\psi = \frac{2\pi}{\lambda}\frac{D}{L}\Delta x_{beam} \quad (7)$$

where Δx_{beam} is the beam offset from the orbit. If the beam moves horizontally from $-\Delta x$ to Δx, the phase shift of the interference pattern will change from $-\Delta\psi$ to $\Delta\psi$. By integrating the interference intensities over this phase shift, we find the averaged visibility:

$$\bar{\gamma} = \mathrm{sinc}(\Delta\psi)\gamma \quad (8)$$

Assuming Δx=50 μm, we get $\Delta\psi$=0.26 and $\bar{\gamma}$ =0.989γ. This 1.1% visibility change only yields less than 1% error in the horizontal beam size (1~2 μm).

As shown in Fig. 2c, the measured visibility has an error bar ±0.01 at fixed slit separation and constant current. This measurement error may come from the fitting error, noise of the CCD camera, and beam jitter. This visibility change ($\Delta\gamma$~0.01) then results in a measured beam size error $\Delta\sigma_x$ for different double slits. As shown in Fig. 4, the beam size error is less than 5 μm when the measured visibility is in the range of 0.2-0.8

(the beam size in the range of 50-400 μm for D=2.0 mm double slits).

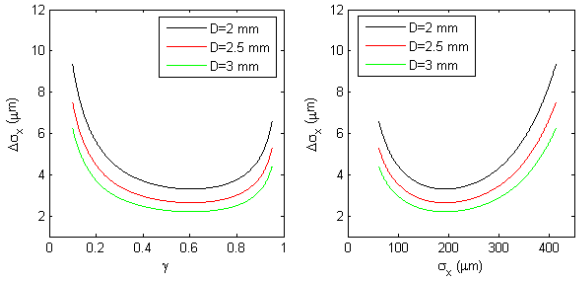

Figure 4: Beam size error as a function of γ and σ_x.

HORIZONTAL EMITTANCE

By measuring the horizontal beam size and knowing the Twiss parameters at the SR source point, we can infer the horizontal emittance ε_x of the CESR-TA low emittance lattice. The measured ε_x is 5.9 nm, which is more than two times larger than the designed (2.6 nm). In order to verify the measurements, we created special knobs which could vary β_x and η_x respectively at the source point without affecting the ε_x of the lattice.

As shown in Fig. 5 (left), with a constant beam current (1mA), the horizontal beam size change followed the change of β_x. From a linear fit of σ_x^2 vs β_x, the horizontal emittance ε_x was extracted as 6.0 nm. Shown in Fig. 5 (right), by increasing the horizontal dispersion η_x at the source point without changing β_x (9.2 m), we also observed the increase of horizontal beam size at a constant beam current (0.6 mA), and σ_x^2 changed quite linearly with the increase of η_x^2. From a linear fit, both the energy spread and emittance were obtained. The measured σ_E/E=0.08% is very close to the design value (0.081%) while the obtained ε_x=5.7 nm is again much larger than the design value.

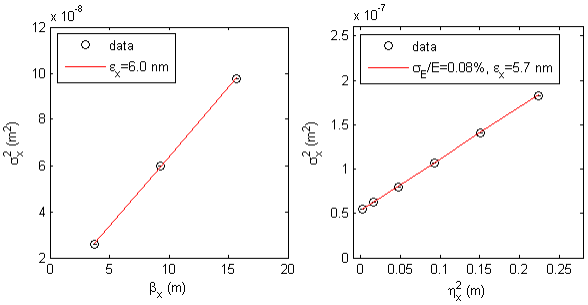

Figure 5: Horizontal beam size vs β_x and η_x.

There are a number of possible explanations for the discrepancy between measured and theoretical horizontal emittance. While the dispersion in the damping wigglers is nominally zero, there may be some residual uncorrected horizontal dispersion in the region of the wigglers. We are also investigating the possibility that the finite dispersion in the RF cavities may be contributing to the effective horizontal beam emittance. Careful measurement and correction of horizontal dispersion will likely help us identify the source of the anomalously large horizontal emittance.

INTRABEAM SCATTERING

The CCD camera settings in our interferometer can be adjusted in real time during measurements. The sensitivity of our camera also allows us to measure the horizontal beam size accurately at very low beam current down to 0.1 mA. We have successfully measured the dependence of horizontal beam size on bunch current during a beam current decay to study IBS.

Figure 6 shows a typical measurement of the horizontal beam size as a function of beam current. We see that the IBS simulation is in reasonable agreement with the experimental data, indicating the horizontal beam size is IBS-dominated. Detailed discussion of IBS can be found in this proceeding [8].

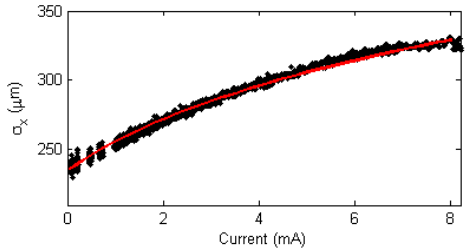

Figure 6: Horizontal beam size as a function of current.

ACKNOWLEDGMENT

The authors thank J.W. Flanagan, M. Billing, J. Shanks, M. Ehrlichman, and W. Hartung for valuable discussions.

REFERENCES

[1] G. Kube, "Review of synchrotron radiation based diagnostics for transverse profile measurements," Proc. of DIPAC 2007, Venice, Italy, 6.

[2] D. Rubin et al., "CesrTA layout and optics," Proc. of PAC 2009, Vancouver, Canada, 2751.

[3] J.A. Clarke, "A review of optical diagnostics techniques for beam profile measurements," Proc. of EPAC 1994, London, England, 1643.

[4] T. Mitsuhashi, Proc. of the Joint US-CERN-Japan-Russia School on Particle Accelerators, Montreux, May 1998, pp. 399-427.

[5] T. Mitsuhashi, "Twelve years of SR monitor development at KEK," Proc. of BIW 2004, Knoxville, USA, CP732.

[6] T. Naito et al., "Very small beam-size measurement by a reflective synchrotron radiation interferometer," Phy. Rev. ST Accel. Beams, 9, 122802 (2006)

[7] J.W. Flanagan et al., "A simpler method for SR interferometer calibration," Proc. of EPAC 2006, Edinburgh, Scotland, 1136

[8] M. Ehrlichman et al., "Intrabeam Scattering studies at CESRTA," WEPPR015, these proceedings.